

# Optical and THz Broadband Integrated Circuits for Mode-Dependent Free-Space Communications

Alan E. Willner

University of Southern California, Dept. of Electrical & Computer Engineering, Los Angeles, CA 90089-2565, USA  
willner@usc.edu

**Abstract:** Integrated circuits may be important role in future mode-dependent free-space communications. This presentation will describe broadband optical and THz structures that can generate data-carrying beams on unique spatial modes. One example is tunable pixel-array-based metasurfaces. © 2024 A.E. Willner

## 1. Introduction

There is growing interest in high-capacity free-space communication links for various applications [1]. This is true for communication systems in both the optical and terahertz (THz) regimes [2–5]. When compared to radio systems, optical beams typically have higher capacity and directionality, and as well as a lower probability of intercept [2,3]. THz systems, especially near the carrier-wave frequency of  $\sim 300$  GHz, tend to have: (i) higher capacity as compared to millimeter-waves, and (ii) better resilience to atmospheric turbulence as compared to optics [4,5].

Importantly, aggregate data transmission rate for both optical and THz free-space communication systems can be enhanced by using mode-division-multiplexing (MDM), which is a subset of space-division-multiplexing (SDM) [6,7]. In MDM systems, multiple data-carrying beams are simultaneously transmitted through the same medium, and each beam is located on an orthogonal spatial mode from a modal basis set [7]. These beams can be multiplexed at the transmitter, spatially co-propagate, and demultiplexed at the receiver – all with little inherent crosstalk [7]. The modal basis set can be various types, including Laguerre Gaussian ( $LG_{l,p}$ ) and Hermite Gaussian ( $HG_{m,n}$ ) [8–11], and a subset of LG modes that have been demonstrated in optical and THz communication systems are orbital-angular-momentum (OAM) modes [12–15]. OAM beams can be characterized by the following: (i) the phasefront “twists” in a helical fashion as it propagates, (ii) the OAM value,  $l$ , is the number of  $2\pi$  phase shifts in the azimuthal direction, (iii) the intensity profile has rings with a central null, and (iv) the value  $p$  is the number of rings minus 1. Besides multiplexing, modes can also be used for data encoding, such that each symbol can be encoded/transmitted on one of many unique modes [15].

As with many communication systems, photonic and THz integrated circuits (PIC and TIC) may play an important role in the future deployment of mode-dependent communication systems. Potential advantages over using many discrete components include smaller size, lower cost, lower loss, and higher yield [16,17]. A specific type of integrated circuit is one that can generate a desired spatial mode for a given data-carrying beam [18–27]. Potentially desirable characteristics for such a mode-generating integrated circuit include the following:

- (a) **Broadband:** If the integrated circuit operates on waves that cover a wide frequency range, then there are fewer constraints on the wave sources and there is the ability to incorporate the multiplexing of multiple wavelength/frequency channels on top of the existing mode multiplexing [20–25].
- (b) **Tunable:** If the integrated circuit can be tuned to emit different modes from the same source, then various advanced switching and routing functions can be accommodated in the communication system [22,26,27].
- (c) **Multiplexing:** If a single integrated circuit can emit multiple data channels simultaneously and co-axially, then the emitter can also function efficiently as a mode multiplexer; when operated in reverse, a similar circuit may also function as a mode demultiplexer [18,19,24,25].

This presentation will describe various optical and THz integrated circuits that have the potential to enable the above characteristics for mode-dependent free-space communications. Performance results will be described, including modal purity, crosstalk, multi-channel operation, and system penalties.

## 2. Broadband and Tunable Structures

One example of an integrated circuit that can emit a beam on a single spatial mode is a pixel-array-based metasurface [21]. The metasurface is fed by a waveguide that carries a data-modulated beam [21], and the metasurface is designed so that a specific spatial mode is emitted normally to the surface depending on the direction

from which the waveguide meets the metasurface [21]. Moreover, this metasurface can operate in the optical and THz domains [21,22,24,25]. Importantly, this metasurface has been shown to enable the above desirable characteristics of broadband operation, tunable mode emission, and co-axial mode (de)multiplexing [21,22,24,25].

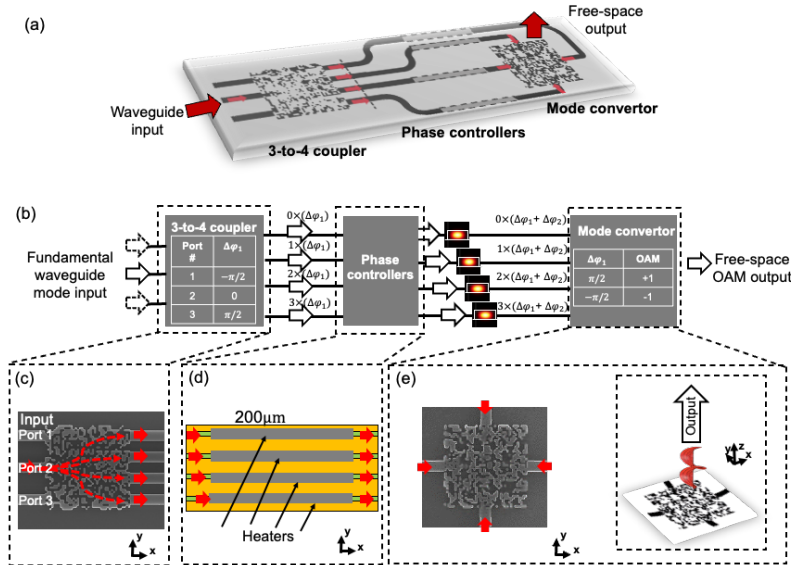


**Fig. 1:** (a) Diagram of an optical pixel-array-based metasurface OAM emitter. (b) The emitter is composed of a passive pixel-array-based 3-to-4 coupler, four tunable phase controllers, and a pixel-array-based mode converter. The OAM order of the data-carrying output beam is dependent on the phase delay induced by the 3-to-4 coupler and the tunable phase controllers. (c) Scanning electron microscopy (SEM) image of the 3-to-4 coupler. (d) Integrated thermal phase controllers. (e) SEM image of the mode converter [22].

A structure to be highlighted is a broadband optical metasurface-based integrated circuit as shown in Fig. 1 [22]. The pixel-array-based metasurface is a mode converter, which converts the mode propagating in an optical waveguide into a different free-space mode that is emitted from the surface [22]. This metasurface is fed by multiple (e.g., four) different optical waveguides that each carry the same data-carrying wave but with a tunable temporal phase delay between each waveguide input into the metasurface. By tuning the phase differential between the waveguides (e.g., by changing the voltage on a set of heaters), the emitted mode can be tuned. Moreover, if there is a couple with multiple input ports and multiple output ports feeding the waveguides, then multiple tunable modes can be emitted simultaneously from the metasurface. Such a structure has also been demonstrated in a reverse way as a mode demultiplexer at receiver for an MDM free-space optical link [24].

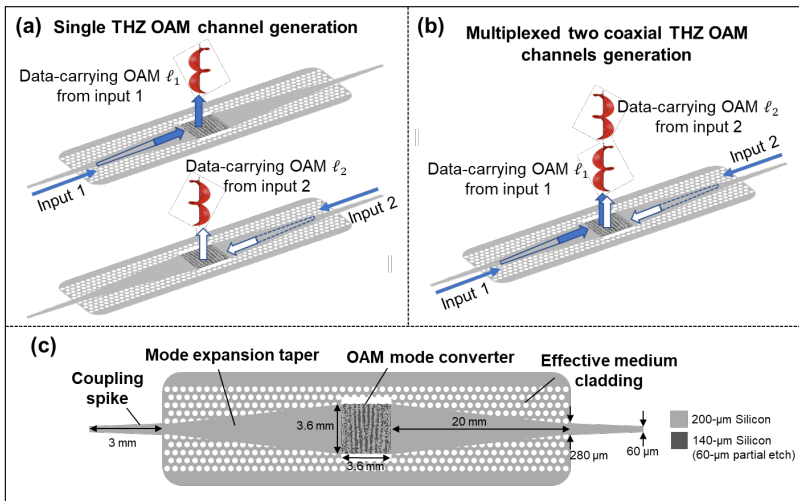


**Fig. 2:** Diagram of a THz pixel-array-based metasurface OAM emitter composed of a mode converter fed by two waveguides from opposite directions. (a) The emitter generates a data-carrying THz OAM beam when a signal is input from one waveguide. (b) The emitter can generate two coaxially multiplexed OAM beams with different orders when signals are input from different waveguides. (c) Schematic of the emitter [25].

Another structure to be highlighted is a broadband THz metasurface-based integrated circuit as shown in Fig. 2 [25]. This THz structure is quite similar to the optical version but with some differences. This broadband structure has two waveguides feeding the THz waves into the metasurface region from opposite directions, and the frequencies of the carrier waves are in the 300-GHz range. The mode of the surface-normal emitted THz beam depends on the direction from which the mode converter metasurface is being fed. Moreover, if two different waves are feeding the converter from different directions, then two different modal beams can be emitted simultaneously. Differences exist between this structure and the optical version, including: (i) the THz structure is larger given the smaller frequency of operation; and (ii) no tunability was designed into the structure, although in theory that could have been included.

### 3. References

1. M. A. Khalighi and M. Uysal, "Survey on free space optical communication: A communication theory perspective," *IEEE Communications Surveys & Tutorials* **16**, 2231–2258 (2014).
2. A. Trichili, M. A. Cox, B. S. Ooi, and M.-S. Alouini, "Roadmap to free space optics," *JOSA B* **37**, A184–A201 (2020).
3. H. Hemmati, *Near-Earth Laser Communications* (CRC press, 2020).
4. C. Chaccour, M. N. Soorki, W. Saad, M. Bennis, P. Popovski, and M. Debbah, "Seven defining features of terahertz (THz) wireless systems: A fellowship of communication and sensing," *IEEE Communications Surveys & Tutorials* **24**, 967–993 (2022).
5. T. Nagatsuma, G. Ducournau, and C. C. Renaud, "Advances in terahertz communications accelerated by photonics," *Nature Photonics* **10**, 371–379 (2016).
6. P. J. Winzer, "Transmission system capacity scaling through space-division multiplexing: a techno-economic perspective," in *Optical Fiber Telecommunications VII*, A. E. Willner, Ed. Academic Press, 2020, pp. 337–369.
7. G. Li, N. Bai, N. Zhao, and C. Xia, "Space-division multiplexing: the next frontier in optical communication," *AOP* **6**, 413–487 (2014).
8. A. M. Yao and M. J. Padgett, "Orbital angular momentum: origins, behavior and applications," *AOP* **3**, 161–204 (2011).
9. A. Forbes, M. de Oliveira, and M. R. Dennis, "Structured light," *Nature Photonics* **15**, 253–262 (2021).
10. K. Pang, H. Song, Z. Zhao, R. Zhang, H. Song, G. Xie, L. Li, C. Liu, J. Du, A. F. Molisch, M. Tur, and A. E. Willner, "400-Gbit/s QPSK free-space optical communication link based on four-fold multiplexing of Hermite–Gaussian or Laguerre–Gaussian modes by varying both modal indices," *Optics Letters* **43**, 3889–3892 (2018).
11. Z. Hu, Y. Li, D. M. Benton, A. A. Ali, M. Patel, and A. D. Ellis, "Single-wavelength transmission at 1.1-Tbit/s net data rate over a multi-modal free-space optical link using commercial devices," *Optics Letters* **47**, 3495–3498 (2022).
12. J. Wang, J.-Y. Yang, I. M. Fazal, N. Ahmed, Y. Yan, H. Huang, Y. Ren, Y. Yue, S. Dolinar, M. Tur, and A. E. Willner, "Terabit free-space data transmission employing orbital angular momentum multiplexing," *Nature Photonics* **6**, 488–496 (2012).
13. H. Zhou, X. Su, A. Minoofar, R. Zhang, K. Zou, H. Song, K. Pang, H. Song, N. Hu, Z. Zhao, A. Almaini, S. Zach, M. Tur, A. Molisch, H. Sasaki, D. Lee, and A. Willner, "Utilizing multiplexing of structured THz beams carrying orbital-angular-momentum for high-capacity communications," *Optics Express* **30**, 25418–25432 (2022).
14. G. Gibson, J. Courtial, M. J. Padgett, M. Vasnetsov, V. Pas'ko, S. M. Barnett, and S. Franke-Arnold, "Free-space information transfer using light beams carrying orbital angular momentum," *Optics Express* **12**, 5448–5456 (2004).
15. A. E. Willner, K. Pang, H. Song, K. Zou, and H. Zhou, "Orbital angular momentum of light for communications," *Applied Physics Reviews* **8**, 041312 (2021).
16. X. Cai, J. Wang, M. J. Strain, B. Johnson-Morris, J. Zhu, M. Sorel, J. L. O'Brien, M. G. Thompson, and S. Yu, "Integrated compact optical vortex beam emitters," *Science* **338**, 363–366 (2012).
17. P. Miao, Z. Zhang, J. Sun, W. Walasik, S. Longhi, N. M. Litchinitser, and L. Feng, "Orbital angular momentum microlaser," *Science* **353**, 464–467 (2016).
18. T. Su, R. P. Scott, S. S. Djordjevic, N. K. Fontaine, D. J. Geisler, X. Cai, and S. Yoo, "Demonstration of free space coherent optical communication using integrated silicon photonic orbital angular momentum devices," *Optics Express* **20**, 9396–9402 (2012).
19. H. Sasaki, Y. Yagi, R. Kudo, and D. Lee, "Demonstration of 1.44 Tbit/s OAM multiplexing transmission in sub-THz bands," in *2023 IEEE International Conference on Communications Workshops (ICC Workshops)* (IEEE, 2023), pp. 338–343.
20. N. Zhou, S. Zheng, X. Cao, Y. Zhao, S. Gao, Y. Zhu, M. He, X. Cai, and J. Wang, "Ultra-compact broadband polarization diversity orbital angular momentum generator with  $3.6 \times 3.6 \mu\text{m}^2$  footprint," *Science Advances* **5**, eaau9593 (2019).
21. Z. Xie, T. Lei, F. Li, H. Qiu, Z. Zhang, H. Wang, C. Min, L. Du, Z. Li, and X. Yuan, "Ultra-broadband on-chip twisted light emitter for optical communications," *Light: Science & Applications* **7**, 18001–18001 (2018).
22. H. Song, H. Zhou, K. Zou, R. Zhang, K. Pang, H. Song, A. Minoofar, X. Su, N. Hu, C. Liu, R. Bock, S. Zach, M. Tur, and A. E. Willner, "Demonstration of generating a 100 Gbit/s orbital-angular-momentum beam with a tunable mode order over a range of wavelengths using an integrated broadband pixel-array structure," *Optics Letters* **46**, 4765–4768 (2021).
23. Y. Chen, Z. Lin, S. Belanger-de Villers, L. A. Rusch, and W. Shi, "WDM-compatible polarization-diverse OAM generator and multiplexer in silicon photonics," *IEEE Journal of Selected Topics in Quantum Electronics* **26**, 6100107 (2019).
24. H. Song, H. Zhou, K. Zou, R. Zhang, K. Pang, H. Song, X. Su, A. Minoofar, N. Hu, C. Liu, R. Bock, B. Lynn, S. Zach, M. Tur, and A. E. Willner, "Demonstration of recovering orbital-angular-momentum multiplexed channels using a tunable and broadband pixel-array-based photonic-integrated-circuit receiver," *Journal of Lightwave Technology* **40**, 1346–1352 (2022).
25. X. Su, H. Song, H. Zhou, K. Zou, Y. Duan, N. Karapetyan, R. Zhang, A. Minoofar, H. Song, K. Pang, S. Zach, A. F. Molisch, M. Tur, and A. E. Willner, "A THz integrated circuit based on a pixel array to mode multiplex two 10-Gbit/s QPSK channels each on a different OAM beam," *Journal of Lightwave Technology* **41**, 1095–1103 (2022).
26. M. N. Malik, N. Zhang, V. Toccafondo, C. Klitis, M. Lavery, A. Sgambelluri, J. Zhu, X. Cai, S. Yu, G. Preve, M. Sorel, A. Bogoni, and M. Scaffardi, "Tunable orbital angular momentum converter based on integrated multiplexers," *Journal of Lightwave Technology* **39**, 91–97 (2021).
27. H. Song, H. Zhou, K. Zou, R. Zhang, X. Su, K. Pang, H. Song, Y. Duan, A. Minoofar, R. Bock, S. Zach, M. Tur, and A. E. Willner, "Experimental demonstration of generating a 10-Gbit/s QPSK Laguerre-Gaussian beam using integrated circular antenna arrays to tune both spatial indices," in *2022 Conference on Lasers and Electro-Optics (CLEO)* (IEEE, 2022), paper SM2N.2.